Effective Learning with Node Perturbation in Deep Neural Networks

Sander Dalm¹ Marcel van Gerven^{*1} Nasir Ahmad^{*1}

Abstract

Backpropagation (BP) is the dominant and most successful method for training parameters of deep neural network models. However, BP relies on two computationally distinct phases, does not provide a satisfactory explanation of biological learning, and can be challenging to apply for training of networks with discontinuities or noisy node dynamics. By comparison, node perturbation (NP) proposes learning by the injection of noise into network activations, and subsequent measurement of the induced loss change. NP relies on two forward (inference) passes, does not make use of network derivatives, and has been proposed as a model for learning in biological systems. However, standard NP is highly data inefficient and unstable due to its unguided noise-based search process. In this work, we investigate different formulations of NP and relate it to the concept of directional derivatives as well as combining it with a decorrelating mechanism for layer-wise inputs. We find that a closer alignment with directional derivatives together with input decorrelation at every layer significantly enhances performance of NP learning with significant improvements in parameter convergence and much higher performance on the test data, approaching that of BP. Furthermore, our novel formulation allows for application to noisy systems in which the noise process itself is inaccessible.

1. Introduction

Backpropagation (BP) is the workhorse of modern artificial intelligence. It provides an efficient way of performing multilayer credit assignment, given a differentiable neural network architecture and loss function (Linnainmaa, 1970). Despite BP's successes, it requires an auto-differentiation framework for the backward assignment of credit, intro-

ducing a distinction between a forward, or inference phase, and a backward, or learning phase, increasing algorithmic complexity and impeding implementation in (neuromorphic) hardware (Kaspar et al., 2021; Zenke & Neftci, 2021). Furthermore, BP has long been criticized for its lack of biological detail and plausibility (Grossberg, 1987; Crick, 1989; Lillicrap et al., 2016), with significant concerns again being the two separate forward and backward phases, but also its reliance on gradient propagation and the non-locality of the information required for credit assignment.

Alternative algorithms have been put forth over the years, though their inability to scale and difficulty in achieving levels of performance comparable to BP have held back their use. One such algorithm is node perturbation (NP) (Dembo & Kailath, 1990; Cauwenberghs, 1992). In NP, node activations are perturbed by a small amount of random noise. Weights are then updated to produce the perturbed activations in proportion to the degree by which the perturbation improved performance. This method requires a measure of the loss function being optimised on a network both before and after the inclusion of noise. Such an approach is appealing because it leverages the same forward pass twice, rather than relying on two computationally distinct phases. It also does not require non-local information other than the global performance signal.

Despite these benefits, Hiratani et al. (2022) demonstrate that NP is extremely inefficient compared to BP, requiring two to three orders of magnitude more training cycles, depending on network depth and width. In addition, they found training with NP to be unstable, in many cases due to exploding weights. Another phenomenon uncovered in their work is that the covariance of NP's updates is significantly higher than that of BP, which can mathematically be described as an effect mediated by correlations in the input data.

Another proposed approach, referred to as weight perturbation (WP), is to inject noise directly into the weights of a network, rather than the activations (Werfel et al., 2003; Fiete & Seung, 2006). This method shows similarities to evolutionary algorithms and can outperform NP in special cases (Züge et al., 2021). A downside to WP is that there are many more weights than nodes in neural networks, making the exploration space larger thus slowing down learning.

^{*}Equal contribution ¹Donders Institute for Brain, Cognition and Behaviour, Radboud University, Nijmegen, the Netherlands. Correspondence to: Nasir Ahmad <nasir.ahmad@donders.ru.nl>.

In fact, both NP and WP lag far behind BP in terms of efficiency. This is to be expected, however, as noise perturbations conduct a random search through parameter space, rather than being gradient directed.

In this work, we put forward three contributions. First, we reframe the process of node perturbation together with the subsequent measurement of the output loss change in terms of directional derivatives. This provides a more solid theoretical foundation for node perturbation and, consequently, a different update rule, which we refer to as iterative node perturbation. Directional derivatives have been related to NP before in the context of forward gradient learning (Baydin et al., 2022; Ren et al., 2022). This approach is different from ours in that the perturbations are used to estimate gradients, but node-perturbed forward passes are not performed network-wide, making these approaches unsuitable for use in true noisy systems.

Second, we introduce an approximation to iterative node perturbation, referred to as activity-based node perturbation, which is more efficient and has the additional advantage that it can be implemented in noisy systems such as imprecise hardware implementations (Gokmen, 2021) or biological systems (Faisal et al., 2008), where the noise itself is not directly measurable.

Third, we propose to use a decorrelation method, first described by Ahmad et al. (2023), to debias layer-wise activations and thereby achieve faster learning. Because NP-style methods directly correlate perturbations of unit activities with changes in a reward signal, decorrelation of these unit activities helps to eliminate confounding effects, making credit assignment more straightforward. In addition, as demonstrated by Hiratani et al. (2022), correlations in the input data lead to more bias in NP's updates by increasing their covariance. By combining decorrelation with the different NP methods, we find that it is possible to achieve orders of magnitude increase in model convergence speed, with performance levels rivalling networks trained by BP in certain contexts.

2. Methods

2.1. Node perturbation and its formulations

Let us define the forward pass of a fully-connected neural network, with L layers, such that the output of a given layer, $l \in {1,2,\ldots,L}$ is given by $\mathbf{x}_l = f(\mathbf{a}_l)$, where $\mathbf{a}_l = \mathbf{W}_l\mathbf{x}_{l-1}$ is the pre-activation with weight matrix \mathbf{W}_l , f is the activation function and \mathbf{x}_l is the output from layer l. The input to our network is therefore denoted \mathbf{x}_0 , and the output \mathbf{x}_L . We consider learning rules which update the weights of such a network of the form

$$\mathbf{W}_l \leftarrow \mathbf{W}_l - \eta_W \Delta \mathbf{W}_l$$
,

where η_W is a small, constant learning rate, and $\Delta \mathbf{W}_l$ is a parameter update direction for a particular algorithm. Recall that the regular BP update is given by

$$\Delta \mathbf{W}_l = \mathbf{g}_l \mathbf{x}_{l-1}^{\top} \tag{1}$$

with $g_l = \frac{\partial \mathcal{L}}{\partial \mathbf{a}_l}$ the gradient of the loss \mathcal{L} with respect to the layer activations \mathbf{a}_l . Our aim is (1) to derive gradient approximations which have better properties than standard node perturbation and (2) to show that decorrelation massively improves convergence performance for any of the employed learning algorithms. In the following, we consider weight updates relative to a single input sample \mathbf{x}_0 . In practice, these updates are averaged over mini-batches.

2.1.1. Traditional node perturbation

In the most common formulation of NP, noise is injected into each layer's pre-activations and weights are updated in the direction of the noise if the loss improves and in the opposite direction if it worsens. Two forward passes are required: one clean and one noise-perturbed. During the noisy pass, noise is injected into the pre-activation of each layer to yield a perturbed output

$$\tilde{\mathbf{x}}_{l} = f\left(\tilde{\mathbf{a}}_{l} + \epsilon_{l}\right) = f\left(\mathbf{W}_{l}\tilde{\mathbf{x}}_{l-1} + \epsilon_{l}\right), \qquad (2)$$

where the added noise $\epsilon_l \sim \mathcal{N}(\mathbf{0}, \sigma^2 \mathbf{I}_l)$ is a spherical Gaussian perturbation with no cross-correlation and \mathbf{I}_l is an $N_l \times N_l$ identity matrix with N_l the number of nodes in layer l. Note that this perturbation has a cumulative effect on the network output as each layer's perturbed output $\tilde{\mathbf{x}}_l$ is propagated forward through the network, resulting in layers deeper in the network being perturbed by more than just their own added noise..

Having defined a clean and noise-perturbed network-pass, we can measure a loss differential for a NP-based update. Supposing that the loss \mathcal{L} is measured using the network outputs, the loss difference between the clean and noisy network is given by

$$\delta \mathcal{L} = \mathcal{L}(\tilde{\mathbf{x}}_L) - \mathcal{L}(\mathbf{x}_L),$$

where $\delta \mathcal{L}$ is a scalar measure of the difference in loss induced by the addition of noise to the network. Given this loss difference and the network's perturbed and unperturbed outputs, we compute a layer-wise learning signal by replacing the gradient \mathbf{g}_l in Eq. 1 with a term consisting of the normalized noise vector direction and the change in loss

$$\Delta \mathbf{W}_{l}^{\text{NP}} = \frac{\delta \mathcal{L}}{\sigma} \epsilon_{l} \mathbf{x}_{l-1}^{\top}.$$
 (3)

2.1.2. Iterative node perturbation

Though mathematically simple, the traditional NP approach described above has a number of drawbacks. One of the

biggest drawbacks is that each layer's noise impact upon the loss is confounded by additional noise in previous and following layers which is unaccounted for. Appendix A describes how correlations arise between layers. Furthermore, a precise relationship between the traditional NP formulation and gradient descent is missing.

In the following, we develop a more principled approach to node perturbation. Our goal is to determine the gradient of the loss with respect to the pre-activations in a layer l by use of perturbations. To this end, we consider the partial derivative of the loss with respect to the pre-activation \mathbf{a}_l^i of unit i in layer l for all i. We define a perturbed state as $\tilde{\mathbf{x}}_k(h) = f(\tilde{\mathbf{a}}_k + h\mathbf{m}_k)$ with h an arbitrary scalar and binary vectors $\mathbf{m}_k = \mathbf{e}_i$ if k = l with \mathbf{e}_i a standard unit vector and $\mathbf{m}_k = \mathbf{0}$ otherwise. We may now define the partial derivatives as

$$(\mathbf{g}_l)_i = \lim_{h \to 0} \frac{\mathcal{L}(\tilde{\mathbf{x}}_L(h)) - \mathcal{L}(\mathbf{x}_L)}{h}.$$

This suggests that node perturbation can be rigorously implemented by measuring derivatives using perturbations $h\mathbf{m}_k$ for all units i individually in each layer l. However, this would require as many forward-passes as there exist nodes in the network, which would be extremely inefficient.

An alternative approach is to define perturbations in terms of directional derivatives. Directional derivatives measure the derivative of a function based upon an arbitrary vector direction in its dependent variables. However, this can only be accomplished for a set of dependent variables which are individually independent of one-another. Thus, we cannot compute such a measure across an entire network. We can, however, measure the directional derivative with respect to a specific layer via a perturbation given by $\tilde{\mathbf{x}}_k(h) = f(\tilde{\mathbf{a}}_k + h\mathbf{v}_k)$, where $\mathbf{v}_k \sim \mathcal{N}(0, \mathbf{I}_k)$ if k = l and $\mathbf{v}_k = \mathbf{0}$ otherwise. Given this definition, we can precisely measure a directional derivative with respect to the activities of layer l in our deep neural network, in vector direction $\mathbf{v} = (\mathbf{v}_1, \dots, \mathbf{v}_L)$ as

$$\nabla_{\mathbf{v}} \mathcal{L} = \lim_{h \to 0} \frac{\mathcal{L}\left(\tilde{\mathbf{x}}_L(h)\right) - \mathcal{L}\left(\mathbf{x}_L\right)}{h||\mathbf{v}||_2}$$

where the directional derivative is measured by a difference in the loss induced in the vector direction \mathbf{v} , normalized by the vector length and in the limit of infinitesimally small perturbation. Note that this derivative is only being measured for layer l, for all other layers the perturbation vector is composed of zeros.

By averaging the directional derivative across samples of the vector \mathbf{v} , we exactly recover the gradient of the loss with respect to a specific layer, such that

$$\mathbf{g}_l = \sqrt{N_l} \left\langle \nabla_{\mathbf{v}} \mathcal{L} \frac{\mathbf{v}_l}{||\mathbf{v}||_2} \right\rangle_{\mathbf{v}}.$$

Appendix B demonstrates this equivalence.

This method allows us to measure the gradient of a particular layer of a deep neural network by perturbation. However, in practice it remains inefficient given the requirement for averaging over a large number of noise samples and the requirement to carry out perturbations separately for each layer. We refer to this method, with sample-wise weight update

$$\Delta \mathbf{W}_{l}^{\text{INP}} = \sqrt{N_{l}} \, \delta \mathcal{L} \frac{\mathbf{v}_{l}}{||\mathbf{v}||_{2}^{2}} \, \mathbf{x}_{l-1}^{\top}$$
 (4)

as iterative node perturbation (INP).

2.1.3. ACTIVITY-BASED NODE PERTURBATION

Though theoretically grounded, INP incurs significant overhead compared to the direct noise-based update method. Specifically, in order to precisely compute directional derivatives, noise must be applied in a purely layer-wise fashion, requiring a high degree of control over the noise injection. This is less biologically plausible and functionally more challenging implementation with less potential for scaling. Furthermore, the number of forward passes required to compute such an update for a whole network for INP is then the number of layers plus one, L+1, potentially many times larger than simple 2-passes required for NP.

To balance learning speed and computational cost we instead approximate the directional derivative across the whole network simultaneously. This involves assuming that all node activations in our network are independent and treating the entire network as if it were a single layer. This can be achieved by, instead of measuring and tracking the injected noise alone, measuring the state difference between the clean and noisy forward passes of the whole network. Note that this is a significant departure from traditional node perturbation in which access to the underlying noise source is required. Concretely, taking the definition of the forward pass given by NP in Eq. 2, we define

$$\Delta \mathbf{W}_{l}^{\text{ANP}} = \sqrt{N} \ \delta \mathcal{L} \frac{\delta \mathbf{a}_{l}}{||\delta \mathbf{a}||_{2}^{2}} \mathbf{x}_{l-1}^{\top}, \tag{5}$$

where $N = \sum_{l=0}^{L} N_l$ is the number of units in the network, $\delta \mathbf{a}_l = \tilde{\mathbf{a}}_l - \mathbf{a}_l$ is the activity difference between a noisy and clean pass in layer l and $\delta \mathbf{a} = (\delta \mathbf{a}_1, \dots, \delta \mathbf{a}_L)$ is the concatenation of activity differences. The resulting update rule is referred to as activity-based node perturbation (ANP).

Here, we have now updated multiple aspects of the NP rule. First, rather than using the measure of noise injected at each layer, we instead measure the total change in activation between the clean and noisy networks. This aligns our measure more closely with the directional derivative: we truly measure how the network changed in its response rather than ignoring the impact of all previous layers and their noise upon the current layer.

This direct use of the activity difference also requires a recomputation of the scale of the perturbation vector. Here we carry the rescaling out by a normalization based upon the activity-difference length and then upscale the signal of this perturbation based upon the network size.

Note that the ANP rule is now a hybridization of the directional derivative and traditional node perturbation. In the limit where the nodes are not interdependent (i.e. when we have a single layer), it is equivalent to INP and upon averaging across many samples can arbitrarily well approximate the true gradient. When used in a layered network structure, it 'assumes' that all nodes are mutually independent even though they are not. This is the only remaining approximation for this approach and it is desirable to allow whole network learning without direct access to the noise vectors.

2.2. Increasing NP efficiency through decorrelation

Uncorrelated data variables have been proposed and demonstrated as impactful in making credit assignment more efficient in deep neural networks (LeCun et al., 2002). If a layer's inputs, \mathbf{x}_l , have highly correlated features, a change in one feature can be associated with a change in another correlated feature, making it difficult for the network to disentangle the contributions of each feature to the loss. This can lead to less efficient learning, as has been described in previous research in the context of BP (Luo, 2017; Wadia et al., 2021). NP additionally benefits from decorrelation of input variables at every layer. Specifically, Hiratani et al. (2022) demonstrate that the covariance of NP updates between layers k and l can be described as

$$C_{kl}^{\text{np}} \approx 2C_{kl}^{\text{sgd}} + \delta_{kl} \left\langle \sum_{m=1}^{k} \|\mathbf{g}_m\|^2 \mathbf{I}_k \otimes \mathbf{x}_{k-1} \mathbf{x}_{k-1}^T \right\rangle_{\mathbf{x}},$$

where C_{kl}^{sgd} is the covariance of SGD updates, δ_{kl} is the Kronecker delta and \otimes is a tensor product. The above equation implies that in NP the update covariance is twice that of the SGD updates plus an additional term that depends on the correlations in the input data, $\mathbf{x}_{k-1}\mathbf{x}_{k-1}^T$. Removing correlations from the input data should therefore reduce the bias in the NP algorithm updates, possibly leading to better performance.

In this work, we introduce decorrelated node perturbation, in which we decorrelate each layer's input activities using a trainable decorrelation procedure first described by Ahmad et al. (2023). A layer input \mathbf{x}_l is decorrelated by multiplication by a decorrelation matrix \mathbf{R}_l to yield a decorrelated input $\mathbf{x}_l^* = \mathbf{R}_l \mathbf{x}_l$. The decorrelation matrix \mathbf{R}_l is then updated according to

$$\mathbf{R}_{l} \leftarrow \mathbf{R}_{l} - \eta_{R} \left(\mathbf{x}_{l}^{\star} \left(\mathbf{x}_{l}^{\star} \right)^{\top} - \operatorname{diag} \left(\left(\mathbf{x}_{l}^{\star} \right)^{2} \right) \right) \mathbf{R}_{l} \,,$$

where η_R is a small constant learning rate and \mathbf{R}_l is ini-

tialised as the identity matrix. For a full derivation of this procedure see (Ahmad et al., 2023).

Decorrelation can be combined with any of the formulations described in the previous sections by replacing \mathbf{x}_l in Eq. 1 with \mathbf{x}_l^* . We will use DBP, DNP, DINP and DANP when referring to the decorrelated versions of the described learning rules. In Appendix C, Algorithm 1, we describe decorrelation using the activity-based update procedure. Appendix D illustrates the operations carried out to compute updates for the described methods.

2.3. Experimental validation

To measure the performance of the algorithms proposed, we ran a set of experiments with the CIFAR-10 dataset (Krizhevsky, 2009), specifically aiming to quantify the performance differences between the traditional (NP), layer-wise iterative (INP) and activity-based (ANP) formulations of NP. This dataset was chosen as it has previously been shown to yield low performance when training networks using regular node perturbation, demonstrating its limitations (Hiratani et al., 2022).

Experiments were performed using a three-hidden-layer fully-connected neural network with leaky ReLU activation functions and a mean squared error (MSE) loss on the one-hot encoding of class membership. Experiments were repeated using five different random seeds, after which performance statistics were averaged. The learning rates were determined for each algorithm separately by a grid search, in which the learning rate started at 10^{-6} and was doubled until performance stopped increasing. Appendix E reports the learning rates used in the experiments. When using NP methods, activity perturbations were drawn from a univariate Gaussian with variance $\sigma^2 = 10^{-6}$. Appendix F shows that our results do not depend significantly on σ^2 , producing similar results when varying σ^2 by a few orders of magnitude.

Another experiment was run with CIFAR-10 to determine the performance effects of decorrelation. This was done in both a single-layer and a three-hidden-layer network, so that the scaling properties of the algorithms could be studied. Decorrelated BP (DBP) was also added as a baseline for this and subsequent simulations. The specific architectures are described in Appendix G.

Additionally, two scaling experiments were run. One using CIFAR-10 with 3, 6, or 9 fully-connected hidden layers and another one using CIFAR-100 and a convolutional architecture with 3 convolutional layers, followed by a fully-connected hidden layer and an output layer. The purpose of these experiments was to assess whether the algorithms scale to deeper architectures and higher output dimensions. The latter has been shown to be a specific issue for the

traditional NP algorithm (Hiratani et al., 2022).

Finally, an experiment with DNP and DANP was run where two noisy forward passes were used, instead of a clean and a noisy pass. This experiment specifically investigates whether DANP might provide benefits over DNP in inherently noisy systems.

3. Results

3.1. Comparing NP formulations

In single-layer networks, the three described NP formulations (NP, INP and ANP) converge to an equivalent learning rule. Therefore, multi-layer networks with three hidden layers were used to investigate performance differences across our proposed formulations.

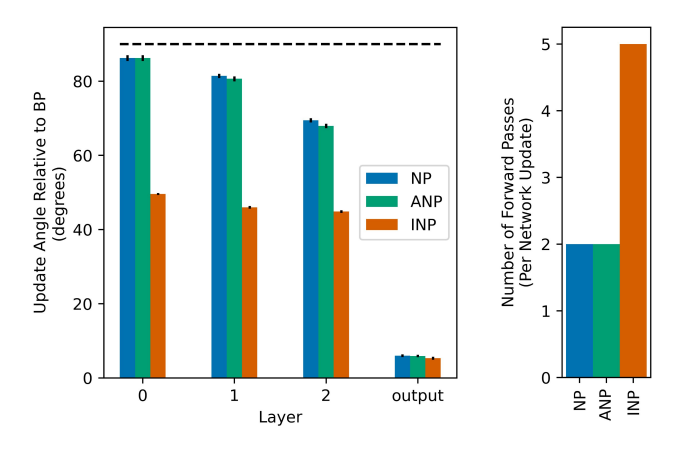


Figure 1. Left, the angles of weight updates (relative to that computed by BP) of the NP, ANP and INP algorithms across the layers of a randomly initialized three hidden layer feedforward network. These angles are measured based on a single mini-batch of size 1000, with 10 random repeats carried out to form the error bars (standard error). Right, the number of forward passes required to compute a single update for each method. For NP and ANP two passes are required for any network update, one clean and one noisy. For INP the number of passes required is the number of layers plus one since each layer is individually perturbed and an additional clean pass is required.

Figure 1, left, shows how weight updates of the different node perturbation methods compare to those from BP in a three-hidden-layer, fully-connected, feedforward networks for the CIFAR-10 classification task. When measuring the angles between the update vectors of various methods, we can observe that the INP method is by far the most well-aligned in its updates with respect to backpropagation, followed by ANP and closely thereafter by NP.

These results align with the theory laid out in the methods section of this work. Note that for all of these algorithms, alignment with BP updates improve when updates are averaged over more samples of noise. Therefore, it is the ranking of the angles between the NP algorithms that is of interest here, not the absolute value of the angle itself, as all angles would improve with more noise samples.

Figure 1, right, shows that the node perturbation methods also differ in how many forward passes are required. Specifically, the INP method carries out an individual noise pass for each layer to isolate the impact of noise and to better approach the BP update. In the following we compare INP to the other node perturbation variantes without accounting for this excess number of forward-passes, but a reader should bear in mind this drawback and consider the added computational complexity of INP.

3.2. Impact of decorrelation

To assess the impact of decorrelation on NP's performance, we studied a single-layer network trained with NP, DNP, BP and DBP. Note that the different formulations of NP are identical in a single-layer networks where there is no impact on activities in the layer from past layers.

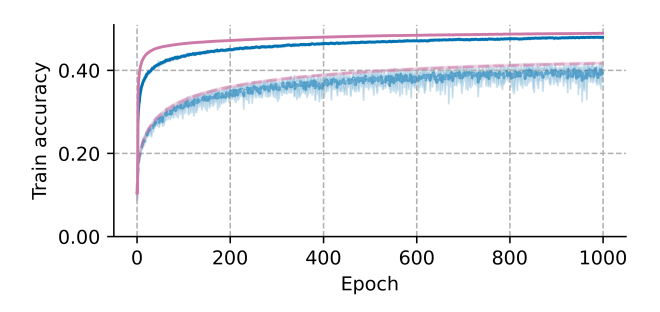
Figure 2 shows that, when training single-layer networks, NP holds up relatively well compared to BP. This is likely due to the limited number of output nodes that need to be perturbed, making NP a decent approximation of BP in this regime. By comparison, DNP converges *faster* than both BP and NP, despite using only a global reward signal. DNP's benefit is less pronounced in test accuracy compared to train accuracy. As in (Ahmad et al., 2023), the benefit of decorrelation for learning was also observed in decorrelated backpropagation (DBP).

It appears that part of the benefit of decorrelation is due to a lack of correlation in the input unit features and a corresponding ease in credit assignment without confound. An additional benefit from decorrelation, that is specific to NP-style updates, is explained by the way in which decorrelation reduces the covariance of NP weight updates, as described in the methods section above.

3.3. Neural network performance comparisons

We proceed by determining the performance of the different algorithms in multi-layer neural networks. See Appendix H for peak accuracies.

Figure 3, shows the various network performance measures when training a multi-layer fully connected network. Though the measured angles during training differ between these algorithms, we can see that this does not appear to have a significant effect in distinguishing the ANP and NP methods. INP does show a performance benefit relative to the other two formulations. Also, all versions of DNP are competitive with BP in terms of train accuracy, with DINP even outperforming BP. For test accuracy, BP remains the



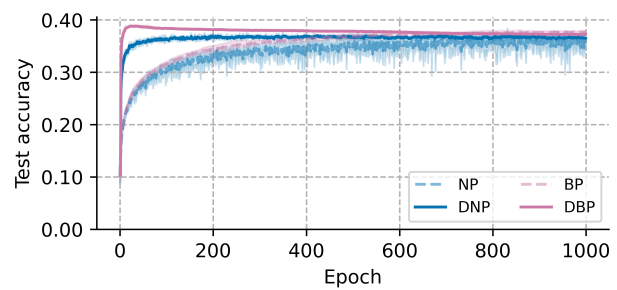
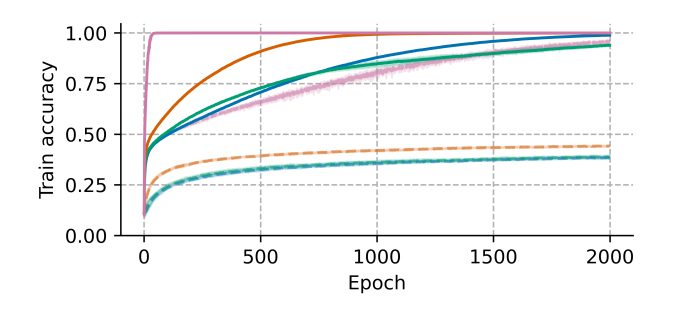


Figure 2. Performance of node perturbation and backpropagation with and without decorrelation on CIFAR-10 when training fully-connected single-layer architecture. Note that all NP methods have an equivalent formulation in a single-layer network.



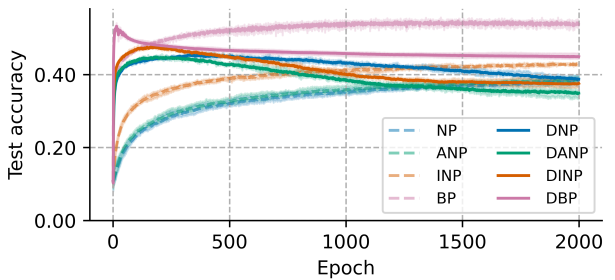


Figure 3. Performance of different NP and BP formulations on CIFAR-10 when training fully-connected three-hidden-layer architectures.

best algorithm and DBP performs by far the best on the train set. Note that DNP performs much better in a three-hidden-layer network than in the single-layer networks explored in Figure 2, meaning that DNP does facilitate multi-layer credit assignment much more than regular NP. To demonstrate that our results generalize to other datasets we report additional results on the SARCOS dataset in Appendix I.

Figure 4 compares the performance of DANP and DINP for 3, 6 and 9 hidden layers. Performance for both algorithms is robust across network depth, with DINP outperforming DANP at every network depth. Though increasing the number of hidden layers beyond three did not boost performance, it also did not make the algorithms unstable, showing potential for the use of DNP in deeper networks. This is an area for future research.

To further investigate the scaling and generalization capacities of our approach, we also trained and tested convolutional architectures for image classification. Figure 5 shows that, when training a convolutional neural network on CIFAR-100, DANP massively outperforms ANP in both train and test accuracy, with DINP performing even better. Both DNP formulations outperform BP on the train set and DINP also outperforms BP on the test set. DBP also outperforms BP, showing the best test performance of all algorithms and catching up with DANP, but not DINP, late in training in terms of train performance.

Note that performance of all algorithms is quite low compared to CIFAR-100 benchmarks as we are using a relatively shallow convolutional neural network in combination with MSE loss, which is not the standard for classification problems with a large output space. The purpose of this experiment was not to attain competitive classification performance per-se, but a comparative study of BP and DNP under a simple training regime. These results also illustrate that the application of such perturbation-based methods can extend beyond fully-connected architectures.

3.4. Node perturbation for noisy systems

One of the most interesting applications of perturbation-based methods for learning are for systems which cannot operate without the possibility of noise. This includes both biological nervous systems as well as a range of analogue computing and neuromorphic hardware architectures. In order to demonstrate that this method is also applicable to architectures with embedded noise, we train networks in which there is no clean network pass available. Instead, two noisy network passes are computed and one is taken as if it were the clean pass. That is, we use $\delta \mathbf{a}_l = \tilde{\mathbf{a}}_l^{(1)} - \tilde{\mathbf{a}}_l^{(2)}$ in Eq . 5. This is similar in spirit to the approach suggested by Cho et al. (2011).

In this case we specifically compare DANP to DNP in terms

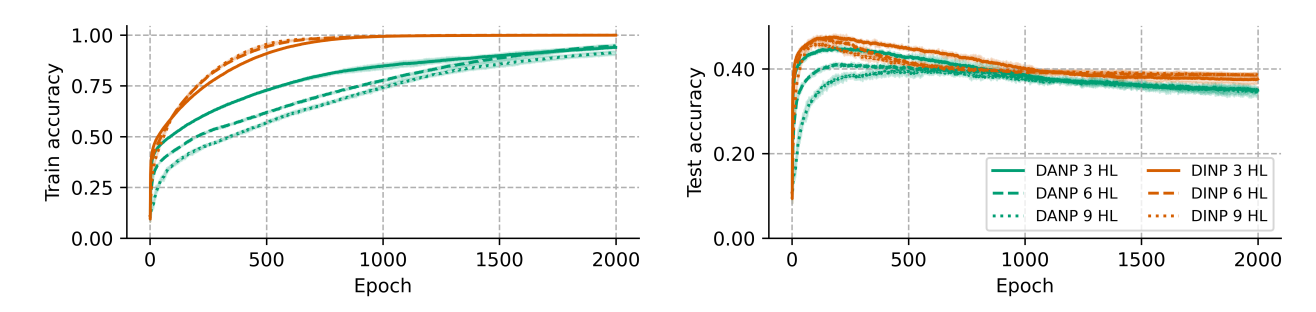


Figure 4. Performance of DANP and DINP for 3-, 6- and 9-hidden-layer networks.

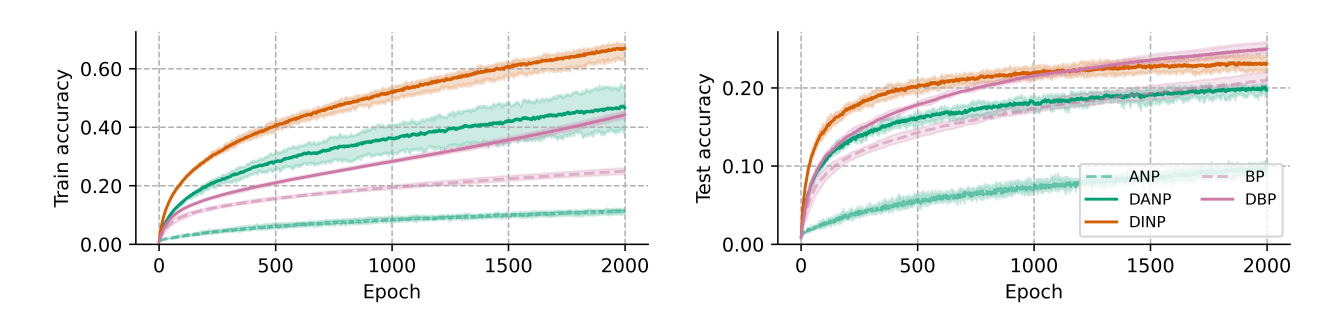


Figure 5. Performance of different node perturbation and backpropagation variants when training a convolutional neural network on CIFAR-100.

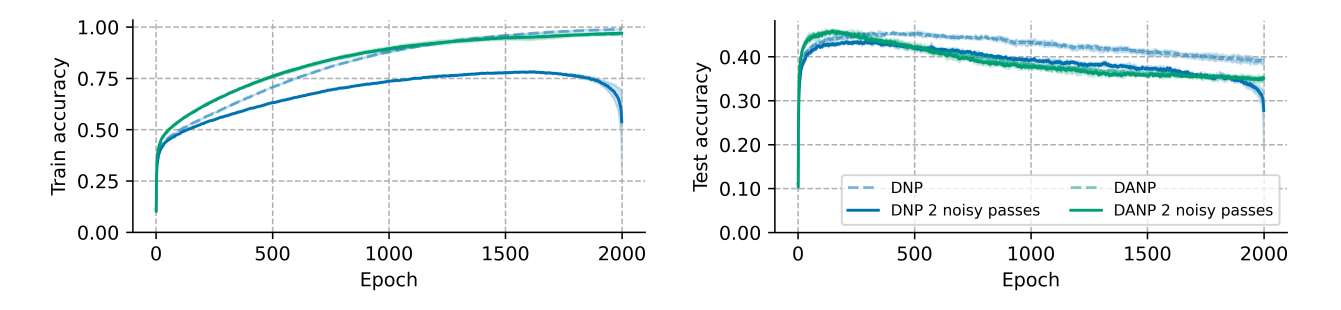


Figure 6. Performance of DANP when applied with one clean network and one noisy network, vs with two noisy network passes. These curves are for a three-layer fully-connected network trained for CIFAR-10 classification (comparable to Figure 3).

of their robustness to a noisy baseline. DANP does not assume that the learning algorithm can independently measure noise. Instead it can only measure the present, and potentially noisy, activity and thereafter measure activity differences to direct learning.

As can be seen in Figure 6, computing updates based upon a set of two noisy passes, rather than a clean and noisy pass, produces extremely similar learning dynamics for DANP with some minimal loss in performance. DNP, by contrast, sees a slowdown in its learning during early training and becomes unstable late in training. It also does not reach the same level of test performance as it does without the noisy baseline. The similarity of the speed of learning and perfor-

mance levels for DANP suggests that clean network passes may provide little additional benefit for the computation of updates in this regime. These results are most promising for application of DANP to systems in which noise is an inherent property and cannot be selectively switched off or read out.

4. Discussion

In this work, we explored several formulations of NP learning and also introduced a layer-wise decorrelation method which significantly outperforms the baseline implementations. In our results we show robust speedups in training

across architectures using the developed learning rules compared to regular NP. This speedup is sufficient to suggest that our alternative formulations of NP could prove to be competitive with traditional BP in certain contexts. We attribute this increased efficacy to a more efficient credit assignment by virtue of decorrelated input features at every layer, as well as an attenuation of the bias in NP's updates caused by their covariance.

The performance of all three methods is substantially improved by including decorrelation. The inclusion of decorrelation does appear to have an impact on the level of overfitting in these systems, with our NP-trained networks having a somewhat lower test accuracy compared to BP. This fits with recent research which suggests an overfitting impact of data whitening (Wadia et al., 2021). In this respect, further investigation is warranted.

When comparing NP, INP and ANP, a number of observations are in order. First, INP yields the best results stemming from its robust relationship to the directional derivative and underlying gradient. The INP method does, however, require running as many forward passes as there are layers in the network (plus one 'clean' pass). This is a drawback for this method and should be considered when analysing its performance, though it should also be considered that it could remain efficient on hardware in which all forward passes are parallelizable. Second, decorrelated variants of NP and ANP both perform well. An additional advantage of the latter though is that one does not need explicit access to the noise vectors, which has important implications for the development of physical learning machines, as described below.

Noise-based learning approaches might also be ideally suited for implementation on neuromorphic hardware (Kaspar et al., 2021). First, as demonstrated in Figure 6, our proposed DANP algorithm scales well even when there is no access to a 'clean' model pass. Furthermore, DANP does not require access to the noise signal itself, in contrast to NP or INP. This means that such an approach could be ideally suited for implementation in noisy physical devices (Gokmen, 2021) even in case the noise cannot be measured. Even on traditional hardware architectures, forward passes are often easier to optimize than backward passes and are often significantly faster to compute. This can be especially true for neuromorphic computing approaches, where backward passes require automatic differentiation implementations and a separate computational pipeline for backward passes (Zenke & Neftci, 2021). In both of these cases, a noise-based approach to learning could prove highly efficient.

Exploring more efficient forms of noise-based learning is interesting beyond credit-assignment alone. This form of learning is more biologically plausible as it does not require weight transport of any kind nor any specific feedback connectivity or computations (Grossberg, 1987; Crick, 1989; Lillicrap et al., 2016). There is ample evidence for noise in biological neural networks (Faisal et al., 2008) and we suggest here that this could be effectively used for learning. Furthermore, the positive impact of decorrelation on learning warrants further investigation of how this mechanism might be involved in neural plasticity. It is interesting to note that various mechanisms act to reduce correlation or induce whitening, especially in early visual cortical areas (King et al., 2013). Additionally, lateral inhibition, which is known to occur in the brain, can be interpreted as a way to reduce redundancy in input signals akin to decorrelation, making outputs of neurons less similar to each other (Békésy, 1967). As described in (Ahmad et al., 2023), decorrelation updates can rely exclusively on information that is locally available to the neuron, making it amenable to implementation in biological or physical systems.

Though the presented methods for effective noise-based learning show a great deal of promise, there are a number of additional research steps to be taken. The architectures considered are relatively shallow, and thus an investigation into how well this approach scales for very deep networks would be beneficial. Testing the scalability of these approaches to tasks of greater complexity is also crucial, as are their application to other network architectures such as residual networks, recurrent networks and attention-based models.

In general, our work opens up exciting opportunities since it has the potential to bring gradient-free training of deep neural networks within reach. That is, in addition to not requiring a backward pass, efficient noise-based learning may also lend itself to networks not easily trained by backpropagation, such as those consisting of activation functions with jumps, binary networks or networks in which the computational graph is broken, as in reinforcement learning.

References

Ahmad, N., Schrader, E., and van Gerven, M. Constrained parameter inference as a principle for learning. *Transactions on Machine Learning Research*, 2023.

Baydin, A. G., Pearlmutter, B. A., Syme, D., Wood, F., and Torr, P. Gradients without backpropagation. *arXiv* preprint arXiv:2202.08587, 2022.

Békésy, G. Mach band type lateral inhibition in different sense organs. *The Journal of General Physiology*, 50: 519–32, 02 1967.

Cauwenberghs, G. A fast stochastic error-descent algorithm for supervised learning and optimization. *Advances in Neural Information Processing Systems*, 5, 1992.

Cho, T., Katahira, K., Okanoya, K., and Okada, M. Node

- perturbation learning without noiseless baseline. *Neural Networks*, 24(3):267–272, April 2011.
- Crick, F. The recent excitement about neural networks. *Nature*, 337:129–32, 02 1989.
- Dembo, A. and Kailath, T. Model-free distributed learning. *IEEE Transactions on Neural Networks*, 1(1):58–70, 1990.
- Faisal, A., Selen, L., and Wolpert, D. Noise in the nervous system. *Nature Reviews. Neuroscience*, 9:292–303, 05 2008.
- Fiete, I. R. and Seung, H. S. Gradient learning in spiking neural networks by dynamic perturbation of conductances. *Physical Review Letters*, 97(4):048104, 2006.
- Gokmen, T. Enabling training of neural networks on noisy hardware. *Frontiers in Artificial Intelligence*, 4:699148, 9 2021. ISSN 26248212. doi: 10.3389/FRAI.2021.699148/BIBTEX.
- Grossberg, S. Competitive learning: From interactive activation to adaptive resonance. *Cognitive Science*, 11:23–63, 1987.
- Hiratani, N., Mehta, Y., Lillicrap, T. P., and Latham, P. E. On the stability and scalability of node perturbation learning. In *Advances in Neural Information Processing Systems*, 2022.
- Kaspar, C., Ravoo, B. J., van der Wiel, W. G., Wegner, S. V., and Pernice, W. H. P. The rise of intelligent matter. *Nature*, 594:345–355, 6 2021.
- King, P. D., Zylberberg, J., and DeWeese, M. R. Inhibitory interneurons decorrelate excitatory cells to drive sparse code formation in a spiking model of V1. *Journal of Neuroscience*, 33(13):5475–5485, March 2013.
- Krizhevsky, A. Learning multiple layers of features from tiny images. Technical report, University of Toronto, 2009.
- LeCun, Y., Bottou, L., Orr, G. B., and Müller, K.-R. Efficient backprop. In *Neural Networks: Tricks of the Trade*, pp. 9–50. Springer, 2002.
- Lillicrap, T. P., Cownden, D., Tweed, D. B., and Akerman, C. J. Random synaptic feedback weights support error backpropagation for deep learning. *Nature Communications*, 7(1):1–10, 2016.
- Linnainmaa, S. The representation of the cumulative rounding error of an algorithm as a Taylor expansion of the local rounding errors. *Master's Thesis (in Finnish), Univ. Helsinki*, pp. 6–7, 1970.

- Luo, P. Learning deep architectures via generalized whitened neural networks. In Precup, D. and Teh, Y. W. (eds.), *Proceedings of Machine Learning Research*, volume 70, pp. 2238–2246, 06–11 Aug 2017.
- Ren, M., Kornblith, S., Liao, R., and Hinton, G. Scaling forward gradient with local losses. *arXiv* preprint *arXiv*:2210.03310, 2022.
- Vijayakumar, S. and Schaal, S. Locally weighted projection regression: An O(n) algorithm for incremental real time learning in high dimensional space. In *Proc. of Seventeenth International Conference on Machine Learning*, pp. 1079–1086, 2000.
- Wadia, N., Duckworth, D., Schoenholz, S. S., Dyer, E., and Sohl-Dickstein, J. Whitening and second order optimization both make information in the dataset unusable during training, and can reduce or prevent generalization. In *International Conference on Machine Learning*, pp. 10617–10629. PMLR, 2021.
- Werfel, J., Xie, X., and Seung, H. S. Learning curves for stochastic gradient descent in linear feedforward networks. Advances in Neural Information Processing Systems, 16, 2003.
- Zenke, F. and Neftci, E. O. Brain-inspired learning on neuromorphic substrates. *Proceedings of the IEEE*, pp. 1–16, 2021. doi: 10.1109/jproc.2020.3045625.
- Züge, P., Klos, C., and Memmesheimer, R.-M. Weight perturbation learning outperforms node perturbation on broad classes of temporally extended tasks. *BioRxiv*, 10 2021.

A. Weights propagate noise correlations

Traditional NP updates have a number of sources of error. One reason is that use of the injected noise ϵ_l to compute the learning signal ignores how the output activity of layer l is not only impacted by the noise injected directly into it, but also by the cumulative effect of perturbations added to previous layers. If the noise is randomly sampled from a Gaussian distribution with mean zero, one might be tempted to simply assume that the perturbations from previous layers cancel out in expectation, but this assumption ignores the correlations introduced into these perturbations by the network's weight matrices at all preceding layers. Multiplying a random vector by a non-orthogonal matrix will introduce a non-random covariance structure into it. To see why, consider a transformation

$$\mathbf{W}\mathbf{x} = \mathbf{y}\,,\tag{6}$$

where W is a randomly initialized weight matrix and x is an uncorrelated input vector for which the following holds in expectation:

$$\langle \mathbf{x} \mathbf{x}^{\top} \rangle = \mathbf{I} \tag{7}$$

with I the identity matrix. The covariance matrix of y can be described as

$$cov_{\mathbf{y}} = \langle \mathbf{y}\mathbf{y}^{\top} \rangle = \langle (\mathbf{W}\mathbf{x})(\mathbf{W}\mathbf{x})^{T} \rangle = \langle (\mathbf{W}\mathbf{x})(\mathbf{x}^{\top}\mathbf{W}^{\top}) \rangle$$
$$= \langle \mathbf{W}\mathbf{x}\mathbf{x}^{\top}\mathbf{W}^{\top} \rangle = \mathbf{W}\langle \mathbf{x}\mathbf{x}^{\top} \rangle \mathbf{W}^{\top} = \mathbf{W}\mathbf{I}\mathbf{W}^{\top} = \mathbf{W}\mathbf{W}^{\top}$$

Therefore, any matrix for which $\mathbf{W}\mathbf{W}^{\top} \neq \mathbf{I}$ will add some covariance structure into output vector \mathbf{y} , even when input vector \mathbf{x} is uncorrelated.

B. The directional derivative as a measure of the gradient

In the main text, we relate the measurement of directional derivatives to the gradient. Specifically, for a feedforward deep neural network of L layers, we state that

$$\mathbf{g}_l = \sqrt{N_l} \left\langle \nabla_{\mathbf{v}} \mathcal{L} \frac{\mathbf{v}_l}{||\mathbf{v}||_2} \right\rangle_{\mathbf{v}},$$

where
$$\mathbf{v} = (\mathbf{v}_1, \dots, \mathbf{v}_L)$$
, and $\mathbf{v}_k \begin{cases} \sim \mathcal{N}(0, \mathbf{I}_k), & \text{if } k = l \\ = \mathbf{0}, & \text{otherwise.} \end{cases}$

Let us now demonstrate the equivalence of the gradient to the expectation over this directional derivative. For simplicity, let us consider a single layer network, such that L=1 and $\mathbf{v}=\mathbf{v}_l=\mathbf{v}_1$. A directional derivative can always be equivalently written as the gradient vector dot product with a (unit-length) direction vector, such that

$$\nabla_{\mathbf{v}} \mathcal{L} = \nabla \mathcal{L}^{\top} \frac{\mathbf{v}}{||\mathbf{v}||_2}.$$

Substituting this form into the above equation requires ensuring that our directional derivative term is no longer treated as a scalar but as a $\mathbb{R}^{1\times 1}$ matrix. We do so below while also removing the now redundant subscripts,

$$\mathbf{g} = \sqrt{N} \left\langle \nabla_{\mathbf{v}} \mathcal{L} \frac{\mathbf{v}^{\top}}{||\mathbf{v}||_{2}} \right\rangle_{\mathbf{v}}^{\top}$$

$$= \sqrt{N} \left\langle \nabla \mathcal{L}^{\top} \frac{\mathbf{v}}{||\mathbf{v}||_{2}} \frac{\mathbf{v}^{\top}}{||\mathbf{v}||_{2}} \right\rangle_{\mathbf{v}}^{\top}$$

$$= \sqrt{N} \left(\nabla \mathcal{L}^{\top} \left\langle \frac{\mathbf{v}\mathbf{v}^{\top}}{||\mathbf{v}||_{2}^{2}} \right\rangle_{\mathbf{v}} \right)^{\top}$$

$$= \sqrt{N} \left\langle \frac{\mathbf{v}\mathbf{v}^{\top}}{||\mathbf{v}||_{2}^{2}} \right\rangle_{\mathbf{v}}^{\top} \nabla \mathcal{L}$$

$$= \sqrt{N} \frac{\sigma^{2} I}{\sigma^{2} \sqrt{N}} \nabla \mathcal{L}$$

$$= \nabla \mathcal{L}.$$

Given our definition of the noise distribution as being composed of independent noise, $\Sigma = \sigma^2 I$, the gradient vector is indeed equivalent to our formulation.

C. Algorithm pseudocode

Algorithm 1 Decorrelated activity-based node perturbation (DANP)

```
Input: data \mathcal{D}, network \{(\mathbf{W}_l, \mathbf{R}_l)\}_{l=1}^L, learning rates \eta_W and \eta_R
for each epoch do
     for each (\mathbf{x_0}, \mathbf{t}) \in \mathcal{D} do
           for layer l from 1 to L do {Regular forward pass}
                 \mathbf{x}_{l-1}^{\star} = \mathbf{R}_{l-1} \mathbf{x}_{l-1}
                \mathbf{a}_l = \mathbf{W}_l \mathbf{x}_{l-1}^{\star}
                \mathbf{x}_l = f(\mathbf{a}_l)
           end for
           for layer l from 1 to L do {Noisy forward pass}
                \tilde{\mathbf{x}}_{l-1}^{\star} = \mathbf{R}_{l-1}\tilde{\mathbf{x}}_{l-1}
                \tilde{\mathbf{a}}_l = \mathbf{W}_l \tilde{\mathbf{x}}_{l-1}^{\star} + \boldsymbol{\epsilon}_l
                \tilde{\mathbf{x}}_l = f(\tilde{\mathbf{a}}_l)
           end for
          \delta \mathcal{L} = (\mathbf{t} - \mathbf{\tilde{x}}_L)^2 - (\mathbf{t} - \mathbf{x}_L)^2 {Compute loss difference}
           for layer l from 1 to L do
                \mathbf{W}_l \leftarrow \mathbf{W}_l - \eta_W \sqrt{N} \, \delta \mathcal{L} \, \frac{\tilde{\mathbf{a}}_l - \mathbf{a}_l}{||\delta \mathbf{a}||_2^2} \left( \mathbf{x}_{l-1}^\star \right)^\top \, \{ \text{Update weight matrix} \}
                \mathbf{R}_{l} \leftarrow \mathbf{R}_{l} - \eta_{R} \left( \mathbf{x}_{l}^{\star} \left( \mathbf{x}_{l}^{\star} \right)^{\mathsf{T}} - \operatorname{diag} \left( \left( \mathbf{x}_{l}^{\star} \right)^{2} \right) \right) \mathbf{R}_{l} \text{ {Update decorrelation matrix}}
           end for
     end for
end for
```

D. Illustration of learning rules

Figure 7 illustrates the difference between different learning rules.

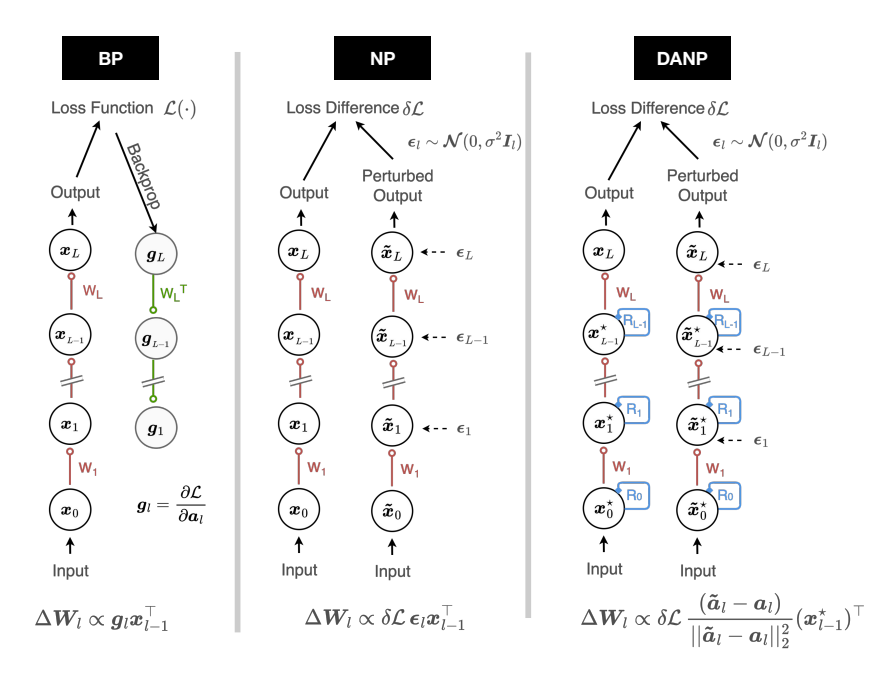


Figure 7. A graphical illustration of the computations required for update measurement for backpropagation (left), node perturbation (middle), and decorrelated activity-based node perturbation (right).

E. Learning rates

Table 1 shows the learning rates η_W used in each experiment. For each experiment, the highest stable learning rate was selected. The search over learning rates started at 10^{-6} and the learning rate was doubled until the highest stable learning rate was found. For the decorrelation learning rate a fixed value of $\eta_R = 10^{-3}$ was chosen based on a prior manual exploration. Note that the minibatch size was fixed for every method at 1000.

Table 1. Learning rates used for different learning algorithms and architectures.

METHOD 1 LAYER		1 LAYER	3 HIDDEN LAYERS	6 HIDDEN LAYERS	9 HIDDEN LAYERS	CONVNET	
	NP	8.2×10^{0}	2.6×10^{-1}	_	_	-	
	DNP	1.0×10^{3}	1.3×10^{2}	_	_	_	
	ANP	_	2.6×10^{-1}	_	_	1.6×10^{1}	
	DANP	_	1.3×10^{2}	6.6×10^{1}	6.6×10^{1}	5.2×10^{2}	
	INP	_	1.0×10^{0}	_	_	_	
	DINP	_	2.6×10^{2}	2.6×10^{2}	2.6×10^{2}	2.1×10^{3}	
	BP	8.0×10^{-6}	6.4×10^{-5}	-	-	5.1×10^{-4}	
	DBP	1.0×10^{-3}	4.1×10^{-3}	-	-	1.0×10^{-3}	
	DBP	1.0×10^{-3}	4.1 × 10	_	-	1.0 × 10	

F. Impact of perturbation scale on performance

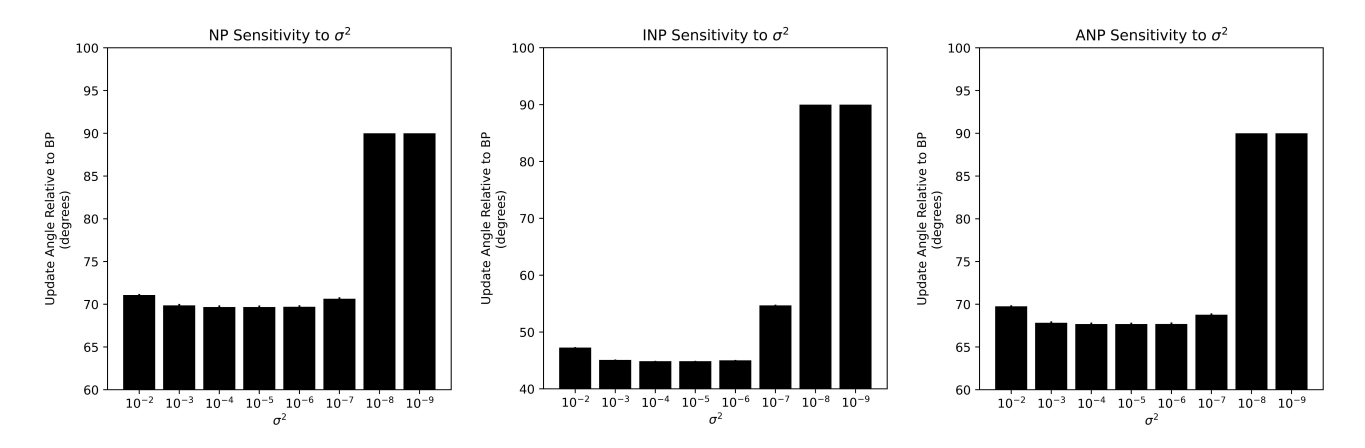


Figure 8. The alignment of NP, INP, and ANP updates measured against BP are shown across a range of perturbation parameters (σ^2). These angles are measure from updates computed for the second hidden layer of a randomly initialized three-hidden layer network being using a 1000 sample mini-batch from the CIFAR-10 dataset. The network from which these are sampled is equivalent to that used in Figure 1.

In all simulations of this paper, random noise is drawn from a set of independent Gaussian distributions with zero mean and some variance, σ^2 . As can be seen in Figure 8, the NP, INP, and ANP methods show a robust performance (when measured based upon alignment with BP updates) to the choice of this variance of the perturbation distribution. For values across multiple orders of magnitude, from 10^{-4} to 10^{-6} , there performance is completely stable. For smaller values of the variance, $\sigma^2 < 10^{-7}$, precision errors cause a decrease in performance (increase in angle). And for larger values of the variance, $\sigma^2 > 10^{-3}$, the size of the perturbation begins to significantly affect network dynamics and thus the approximation of the directional derivative.

In this work we exclusively use $\sigma^2 = 10^{-6}$, the smallest value possible before precision errors become an issue. We do not find significantly different results even if σ^2 is set to be an order of magnitude greater.

G. Neural network architectures

Table 2. Details of the employed neural network architectures consisting of fully connected (FC) and convolutional (Conv) layers. All layers except the output layer are followed by a leaky ReLU transformation.

Network	LAYER TYPES	LAYER SIZE		
SINGLE LAYER	FC	10		
THREE HIDDEN LAYERS	$3 \times FC$	1024		
THREE HIDDEN LATERS	FC	10		
SIX HIDDEN LAYERS	6 × FC	1024		
SIX HIDDEN LATERS	FC	10		
NINE HIDDEN LAYERS	9 × FC	1024		
NINE HIDDEN LATERS	FC	10		
	Conv	3×3×16, 2		
	CONV	$3\times3\times32, 2$		
CONVNET	CONV	$3\times3\times64, 1$		
	FC	1024		
	FC	100		

H. Peak accuracies

Table 3. Peak percentage accuracies for different learning algorithms and architectures. Fully connected models consisting of 1, 3, 6 and 9 hidden layers were trained on CIFAR-10. ConvNets were trained on CIFAR-100. Best performance across all methods is shown in boldface.

	1 LA	TER 3 HIDDEN I		LAYERS 6 HIDDEN LAY		LAYERS	9 HIDDEN LAYERS		CONVNET	
МЕТНОО	TRAIN	TEST	TRAIN	TEST	TRAIN	TEST	TRAIN	TEST	TRAIN	TEST
NP	41.6	38.4	39.2	39.2	l –	_	l –	_	-	_
DNP	48.2	37.5	99.0	46.2	_	-	_	_	-	_
ANP	_	-	39.6	39.7	i –	_	l –	_	12.4	10.7
DANP	_	_	94.6	45.7	95.5	41.6	92.1	40.6	54.9	20.7
INP	_	-	44.5	43.5	_	_	_	_	_	-
DINP	_	-	100.0	48.2	100.0	47.9	100.0	46.8	69.2	24.4
BP	42.0	38.0	96.7	55.7	i –	_	l –	_	26.1	22.0
DBP	49.0	39.0	100.0	54.1	-	-	-	_	45.6	25.9

I. SARCOS experiment

Figure 9 shows train and test loss for (D)NP, (D)ANP and (D)BP on the SARCOS dataset (Vijayakumar & Schaal, 2000). The network was a fully connected architecture with two 32 unit hidden layers and was trained with MSE loss and the leaky ReLU activation function. It was trained for 500 epochs and results were averaged over 3 random seeds. A learning rate search for each algorithm was started at 10^{-7} , doubling the learning rate until the algorithm became unstable. A decorrelation learning rate of 10^{-4} was used for DNP and DANP and 10^{-3} for DBP.

The results indicate that while NP and ANP significantly lag BP in performance, DNP and DANP perform almost as well as BP. Like in other experiments reported in this work, DBP performs best overall. Final test losses were 11.18 (NP), 10.51 (DNP), 15.86 (ANP), 9.79 (DANP), 9.48 (BP) and 7.02 (DBP).

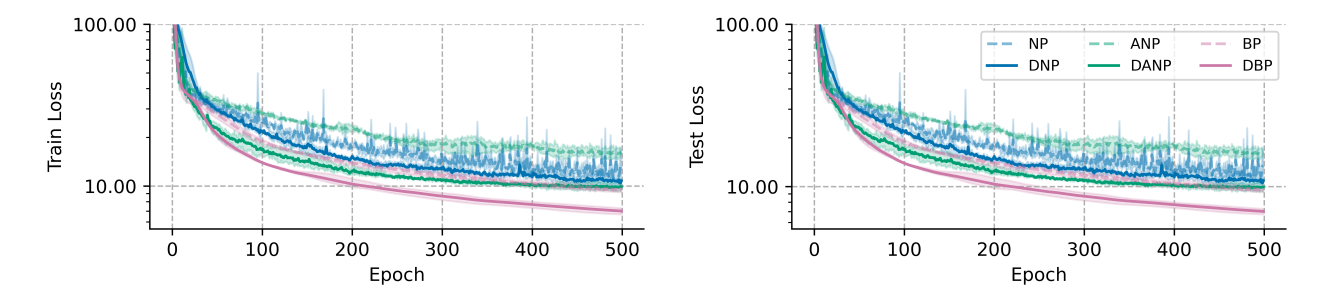


Figure 9. Train and test loss for (D)NP, (D)ANP and (D)BP on the SARCOS dataset. The network was a fully connected architecture with two 32 unit hidden layers and was trained with MSE loss and the leaky ReLU activation function.